Thickness dependence of surface morphology and charge carrier mobility in organic field-effect transistors*

Tian Xue-Yan(田雪雁), Xu Zheng(徐 征)†, Zhao Su-Ling(赵谡玲), Zhang Fu-Jun(张福俊), Yuan Guang-Cai(袁广才), Li Jing(李 婧), Sun Qin-Jun(孙钦军), Wang Yun(王 赟), and Xu Xu-Rong(徐叙瑢)

Institute of Optoelectronic Technology, Beijing Jiaotong University, Beijing 100044, *China*

Key Laboratory of Luminescence and Optical Information (Beijing Jiaotong University), Ministry of Education, Beijing 100044, *China*

(Received 3 April 2009; revised manuscript received 16 July 2009)

With the aim of understanding the relationships between organic small molecule field-effect transistors (FETs) and organic conjugated polymer FETs, we investigate the thickness dependence of surface morphology and charge carrier mobility in pentacene and regioregular poly (3-hexylthiophene) (RR-P3HT) field-effect transistors. On the basis of the results of surface morphologies and electrical properties, we presume that the charge carrier mobility is largely related to the morphology of the organic active layer. We observe that the change trends of the surface morphologies (average size and average roughness) of pentacene and RR-P3HT thin films are mutually opposite, as the thickness of the organic layer increases. Further, we demonstrate that the change trends of the field-effect mobilities of pentacene and RR-P3HT FETs are also opposite to each other, as the thickness of the organic layer increases within its limit.

Keywords: organic field-effect transistors, morphology, thickness dependence, field-effect mobility

PACC: 8115L, 7360R, 8115, 7340T

1. Introduction

Organic field-effect transistors (FETs) based on organic small molecules and conjugated polymers have been envisioned as a viable alternative to more traditional, mainstream field-effect transistors based on inorganic materials. The unique processing characteristics and the demonstrated performance of organic FETs suggest that they can be competitive candidates for existing or novel thin film transistor applications requiring large area coverage, structural flexibility, low temperature processing, and especially low cost. Such applications include smart cards, electronic identification tags, active matrix displays, etc.[1−5]

Organic small molecules such as pentacene, deposited by vacuum sublimation, give the best performance because of their very well ordered structures, resulting from the use of this highly controllable deposition method.[2] But it needs expensive vacuum chambers and lengthy pumpdown cycles. Organic conjugated polymers such as regioregular poly (3-hexylthiophene) (RR-P3HT)[6−10] have a potentially important cost advantage associated with the solution processing of organic TFTs by the reel-to-reel method in the future. However, their mobilities are currently lower than those of vapour deposited pentacene TFTs. Thus, it does not constitute an exclusive advantage for either of the two classes of materials.

The previous studies show that the charge transport properties of organic semiconductors are intimately dependent on their crystal structure and morphologies.[11−13] But these studies focused on the effects of each material in organic FETs. The relationship between organic small molecule FETs and organic conjugated polymer FETs is desired for future device application, which is closely related to the passage from the research laboratory to product development and then to manufacturing of new products based on organic semiconductors. In the present paper, strong dependences of charge carrier mobilities of two types of materials (pentacene and RR-P3HT are used as representatives of organic small molecules and conjugated polymers, respectively) on thickness are revealed, and further, the change trends of field-

*Project supported by the National Natural Science Foundation of China (Grant Nos. 10774013 and 10804006), the National High Technology Research and Development Program of China (Grant No. 2006AA03Z412), the Research Fund for the Doctoral Program of Higher Education of China (Grant No. 20070004024), the Research Fund for the Youth Scholars of the Doctoral Program of Higher Education, China (Grant No. 20070004031), the New Star Plan of Science and Technology of Beijing, China (Grant No. 2007A024) and the research grants from the Academy of Sciences for the Developing World (Grant No. B08002).

†Corresponding author. E-mail: zhengxu@bjtu.edu.cn

© 2010 Chinese Physical Society and IOP Publishing Ltd

effect mobilities of pentacene and RR-P3HT FETs are shown to be mutually opposite, as the thickness of the organic layer increases within its limit.

2. Experiment

2.1. Preparation of pentacene FETs

Pentacene FETs were prepared with bottom-gate and top-contact configuration. A highly doped p-type Si (100) wafer acted as the gate electrode, on which a 250 nm-thick SiO_2 layer was thermally grown as a gate insulator. Then, pentacene thin films at various thicknesses (20 nm, 30 nm, 40 nm and 50 nm) were thermally evaporated at a low deposition rate ($\sim$0.03 nm/s) and a base pressure of 2×10^{-3} Pa. The pentacene was purchased from J & K Chem. Co. with 98% purity, and it was used without repurification. Then, the pentacene thin films were annealed at 90°C for 2 h. Finally, gold (Au) was thermally evaporated to a thickness of 150 nm and used as the drain and the source electrodes through a shadow mask. The channel length (L) and width (W) were 25 μm and 1000 μm, respectively.

2.2. Preparation of RR-P3HT FETs

RR-P3HT FETs were also prepared with bottom-gate and top-contact configuration. The gate insulator layer SiO_2 with 250 nm thickness was prepared by electron beam evaporation at a deposition rate ($\sim$1 Å/s) on pre-cleaned indium tin oxide (ITO) glass substrates. ITO was used as the gate electrode. Then, RR-P3HT thin films were prepared by spin-coating RR-P3HT chloroform solutions (0.5 wt%, 1 wt%, 1.5 wt%, and 2 wt%) at a rate of 2000 r/min for 60 s. Thin films with average thicknesses of about 70 nm, 120 nm, 220 nm and 270 nm were obtained at four different concentrations, i.e. about 0.5 wt%, 1 wt%, 1.5 wt%, and 2 wt%, respectively. Films thicknesses were measured by a step profilometer (AMBIOS-XP2). RR-P3HT was purchased from Sigma–Aldrich with a head-to-tail regiospecific conformation greater than 98.5% and average molecular weight M_n $\sim$64000. The RR-P3HT thin films were annealed at 90 °C under vacuum atmosphere for 10 min. Subsequently, samples were placed under vacuum for 20 h to enhance local self-organization. Finally, the drain and the source electrodes were prepared like the pentacene FETs. The channel length and width are fixed like the pentacene FETs.

2.3. Characterization of samples

The film surface morphology was investigated by atomic force microscopy (AFM) operated in tapping mode (DI Dimension 3100 manual). A good surface image was obtained only in tapping mode due to the softness of the organic film surface. The electrical characteristics were performed by using a Keithley semiconductor parameter analyser (Keithley 2612) at room temperature in air and darkness. In this measurement, organic FETs operated in the accumulation mode by appling negative gate bias, where the source electrode was grounded and the drain electrode was negatively biased.

3. Results and discussion

3.1. Surface morphology of the organic active layer

The nature of charge carriers and their role in charge transport may largely be related to the morphology of the system.[11−13] A detailed study on pentacene thin films at various thicknesses was carried out by using AFM. The surface morphologies of pentacene thin films annealed at 90 °C for 2 h, with four different deposition thicknesses, i.e. 20 nm, 30 nm, 40 nm, and 50 nm, are shown in Figs. 1(a), 1(b), 1(c) and 1(d), respectively. The average grain size decreases from 1500 nm to 200 nm, which represents an increased portion of grain boundaries with thin film thickness increasing from 20 nm to 50 nm. Furthermore, the average roughness of the thin films decreases from 6.009 nm to 4.412 nm with thin film thickness increasing from 20 nm to 50 nm. We check the section analysis spectrum of the surface morphology of pentacene thin film along the indicated line across the image in Fig. 2. The surface distance, the horizontal distance, the vertical distance, and the spectral root-mean-square amplitude (RMS amp) are 24.176 nm, 23.438 nm, 1.455 nm, and 3.387 nm, respectively. As can be seen from the section analysis of the film, the pentacene film shows a typical terrace shape, and these grains

have a layered structure with a monomolecular step height of approximately 1.5 nm. The increase of deposited thickness of pentacene thin film after being annealed leads the density of grain boundaries and the number of grains to increase. Furthermore, there is a possibility that the growth interspace of grains decreases with the increase of deposited thickness during annealing. If the grain boundaries are formed in the layer grown, they will limit the mobility of grains.[14] Therefore, the field effect mobility is expected to decrease with the increase of deposited thickness of pentacene thin film after being annealed.

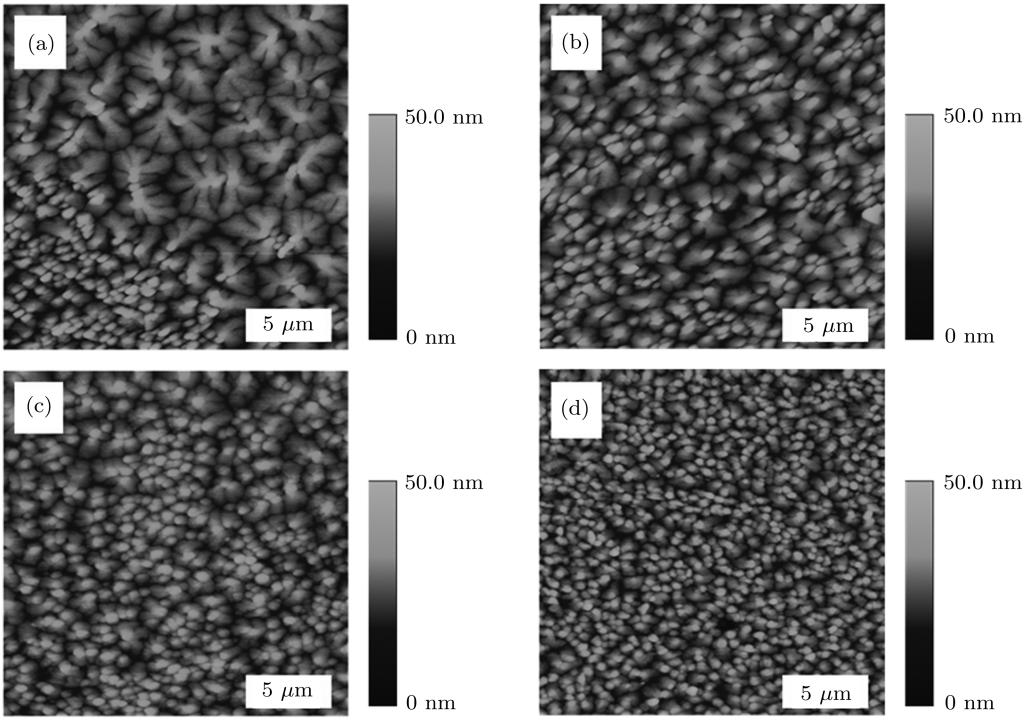


Fig. 1. AFM images of pentacene thin films after being annealed at 90°C for 2 h. The four different deposition thicknesses are (a) 20 nm, (b) 30 nm, (c) 40 nm and (d) 50 nm.

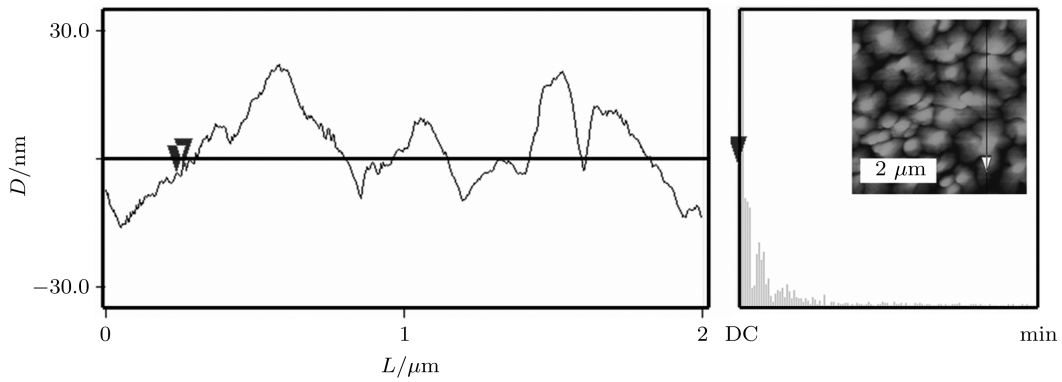


Fig. 2. Section analysis spectrum of the surface morphology of 40 nm-thick pentacene thin film after being annealed at 90°C for 2 h.

Figure 3 shows the AFM images of RR-P3HT thin films annealed at 90 °C, with various thicknesses. We can observe that the average size of islands of RR-P3HT thin films increases from approximately 70 nm to 160–200 nm with thin film thickness increasing from 70 nm to 270 nm. Further, the average roughness is also enhanced gradually from 0.681 nm, 0.724 nm, 2.496 nm, to 4.718 nm as thin film thickness increases. We find that different thicknesses result in distinctly different nanoscale islands. It is expected that the size of the nanoscale islands will play an important role in field-effect mobility.[15,16]

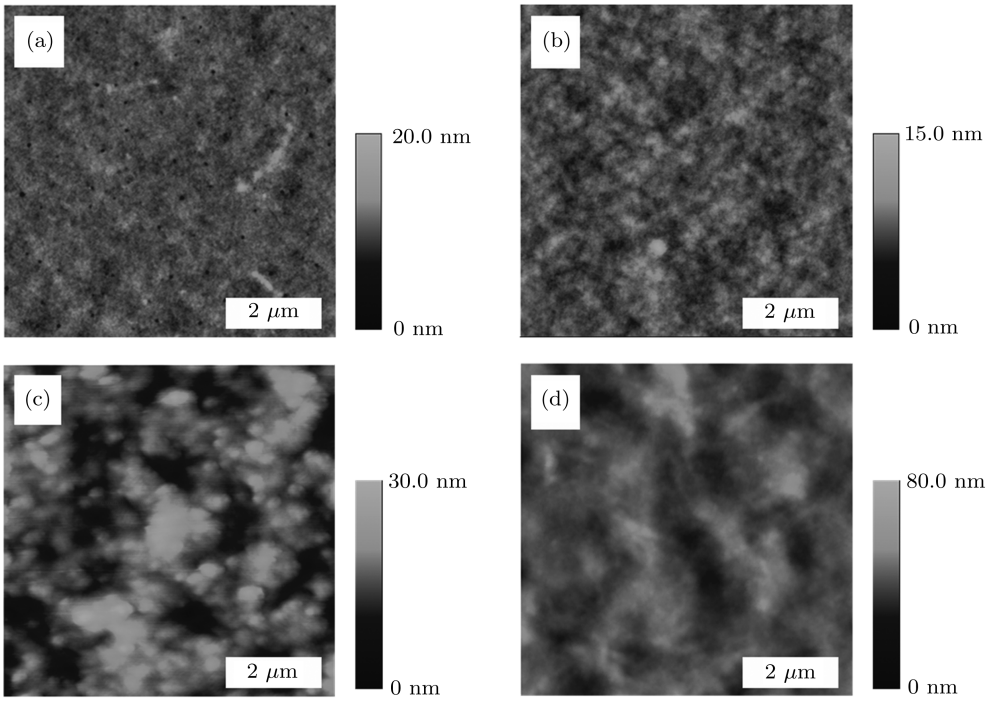


Fig. 3. AFM images of RR-P3HT thin films annealed at 90 °C, with various thicknesses, i.e. about (a) 70 nm, (b) 120 nm, (c) 220 nm and (d) 270 nm.

It seems that the change trends of the surface morphologies (the average size and the average roughness) of pentacene and RR-P3HT thin films are mutually opposite, as the thickness of the organic layer increases. Therefore, the change trends of field-effect mobilities of pentacene and RR-P3HT FETs are expected to be opposite to each other, as the thickness of the organic layer increases within limits.

3.2. Transistor properties

The curves for typical p-type drain current ($I_{\rm DS}$) versus source–drain voltage ($V_{\rm DS}$) at several different gate–source voltages ($V_{\rm GS}$) for pentacene FETs and four deposition thicknesses are shown in Fig. 4. In our experiment, tuning of the work function of gold source and drain electrodes with a modification was not performed. Thus, there is a partial injection barrier of the hole, which manifests itself as an S shaped I–V curve in the early part of the I–V curve (see Figs. 4(a)–4(d)). The field-effect mobility values of pentacene FETs with four different deposition thicknesses are calculated in the saturated regime ($V_{\rm DS} = -10$ V) by plotting the square root of the drain current versus gate voltage and fitting the data to the following equation [17−19]

$$I_{\rm DS} = \frac{\mu W C_i}{2L} (V_{\rm GS} - V_T)^2.$$

Transfer characteristics of the devices are shown in Fig. 5. The detailed characteristics of the devices are summarized in Table 1.

Table 1. The values of field-effect mobility (μ), threshold voltage ($V_{\rm T}$), and on/off current ratio ($I_{\rm on}/I_{\rm off}$) at $V_{\rm DS} = -10$ V in the saturated regime of pentacene FETs after being annealed at 90 °C for 2 h, with four different deposition thicknesses.

organic active layer	average thickness /nm	μ/(cm^2/(V·s))	$V_{\rm T}$/V	$I_{\rm on}/I_{\rm off}$
pentacene	20	0.570	1.4	1.8×10^3
	30	0.263	1.1	7.6×10^2
	40	0.118	1.9	3.7×10^2
	50	0.058	1.2	1.5×10^2

Note: $W/L = 40$ ($W = 1000$ μm and $L = 25$ μm), and 250 nm-thick SiO_2 insulator layer $C_{\rm i} = 10.8$ nF/cm^2.

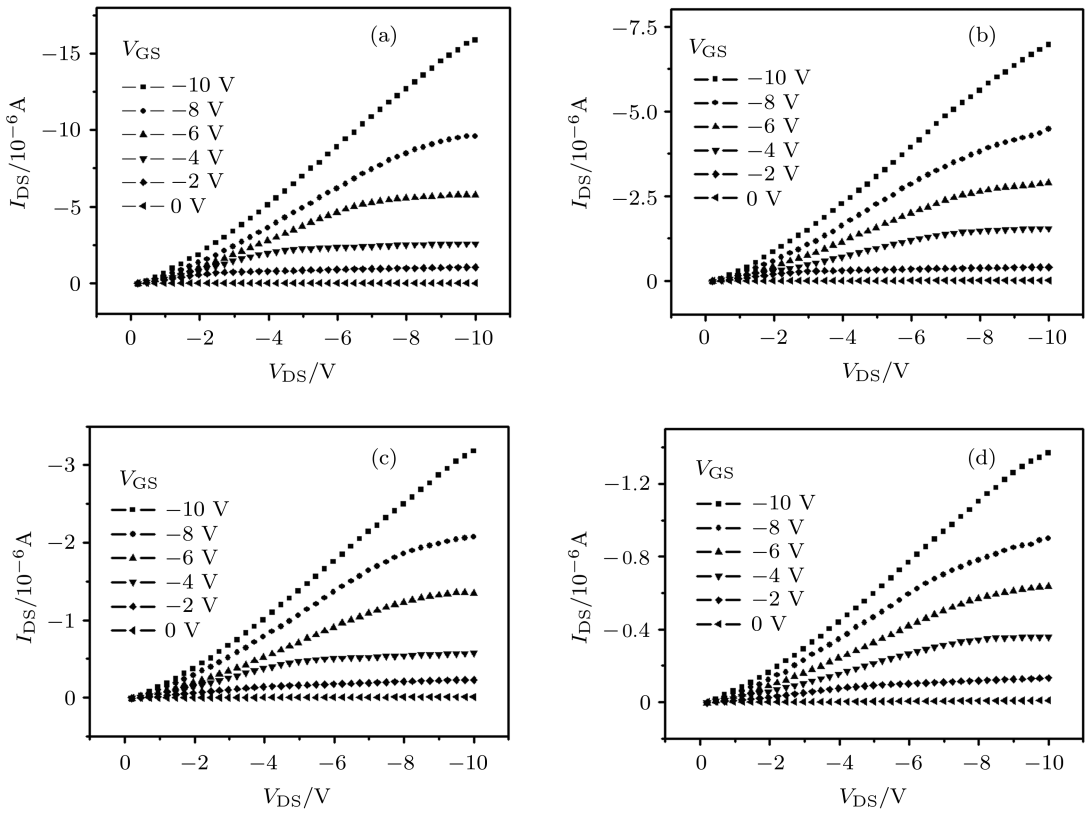


Fig. 4. Output characteristics of pentacene FETs after being annealed at 90 °C for 2 h, with four different deposition thicknesses, i.e. (a) 20 nm, (b) 30 nm, (c) 40 nm and (d) 50 nm.

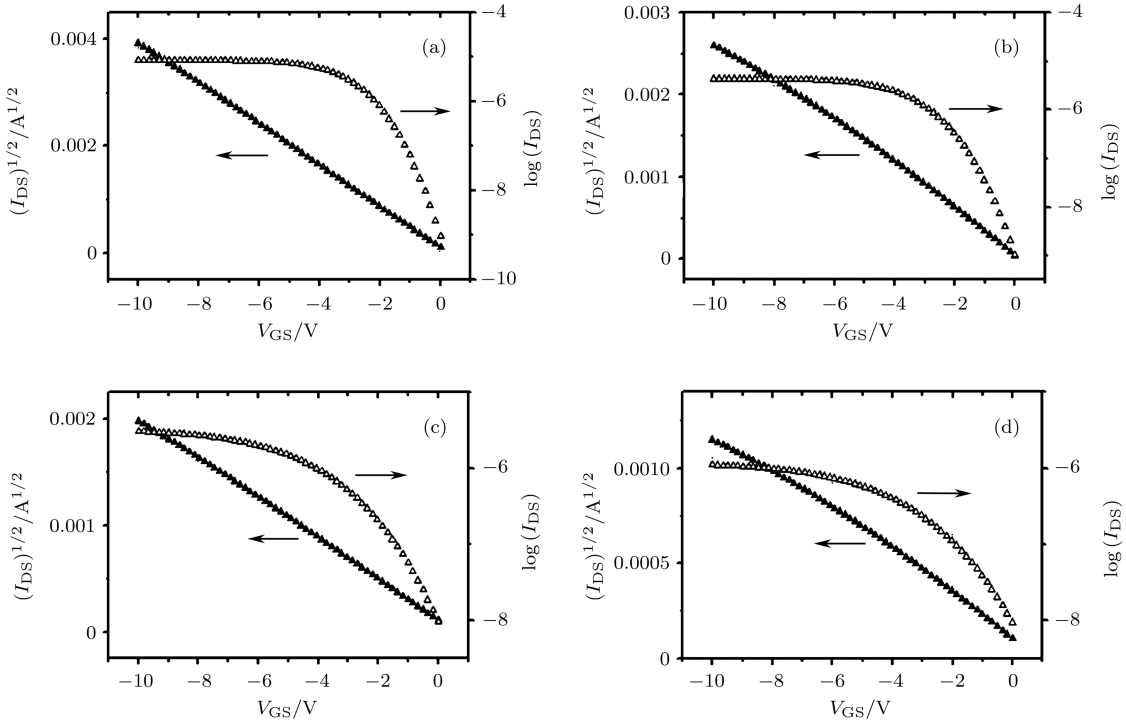


Fig. 5. Transfer characteristics of pentacene FETs after being annealed at 90 °C for 2 h, with four different deposition thicknesses, i.e. (a) 20 nm, (b) 30 nm, (c) 40 nm, and (d) 50 nm and $V_{DS} = -10$ V.

The field-effect mobility values of pentacene FETs at various deposition thicknesses of 20 nm, 30 nm, 40 nm and 50 nm are calculated to be 0.570, 0.263, 0.118 and 0.058, respectively. The results also reveal that the field-effect mobility value of the device with a 20 nm-thick active layer is about one order of magnitude higher than that of the device with a 50 nm-thick active layer. We find that the field-effect mobility and the maximal output drain–source current of pentacene FETs for the $V_{\rm DS} = -10$ V decrease with the increase of deposition thickness, which can be seen from Fig. 6. The values of the on/off current ratio also have a slight decreasing trend with the increase of deposition thickness.

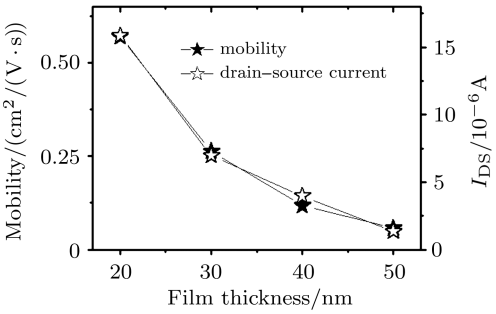


Fig. 6. Thickness dependence of the field-effect mobility and maximal output drain–source current of pentacene FETs for the $V_{\rm DS} = -10$ V.

In a p-channel FET that operated at $V_{\rm T} < 0$, where $V_{\rm T}$ is proportional to the minimum charge needed for channel operation (i.e. the minimum charge needed to fill traps, etc.).[15] This is not the case for our devices due to unpurified source materials and exposure to air. The values of threshold voltage are positive in our experiments. The channel is already conducting even at $V_{\rm GS} = 0$ because of residual p-doping from impurities. In this case, $V_{\rm T}$ is more of an indicator that shows how many positive charges must be compensated before the minimum 'off-current' is reached. If the dopants are movable, then the dopant ions will be repelled from the interface with gate dielectric in the channel when negative $V_{\rm GS}$ is applied.

Transfer characteristics of RR-P3HT FETs annealed at 90 °C with four different thicknesses are presented in Fig. 7, which is in the saturated regime ($V_{\rm DS} = -10$ V) and obtained by plotting the square root of the drain current versus gate voltage. The field-effect mobility values of RR-P3HT FETs with four different active layer thicknesses, i.e. about 70 nm, 120 nm, 220 nm and 270 nm, were similarly calculated to be 4.39×10^{-4}, 7.8×10^{-4}, 5.37×10^{-3} and 5.78×10^{-3}, respectively. We find that the values of field-effect mobility and maximal output drain–source current of RR-P3HT FETs increase drastically with the increase of active layer thickness, which can be seen from Fig. 8. The values of the threshold voltage are around 0 V. Moreover, the values of the on/off current ratio are estimated to be approximately 10^3, and also have a slightly increasing trend with the increase of active layer thickness. Further, we observe that the change trends of field-effect mobilities of pentacene and RR-P3HT FETs are mutually opposite, as the thickness of the organic layer increases within limits. Thus, we presume that the charge carrier mobility is largely related to the morphology of the organic active layer.

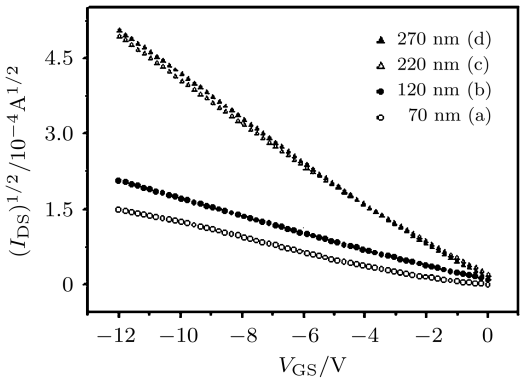


Fig. 7. Transfer characteristics of RR-P3HT FETs annealed at 90 °C with several different thicknesses, i.e. about (a) 70 nm, (b) 120 nm, (c) 220 nm, and (d) 270 nm and $V_{\rm DS} = -10$ V.

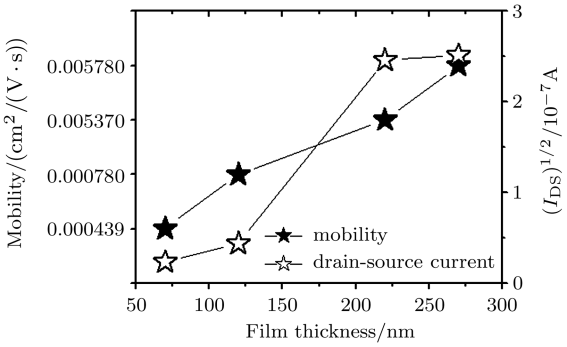


Fig. 8. Thickness dependence of the field-effect mobility and maximal output drain–source current of RR-P3HT FETs for the $V_{\rm DS} = -10$ V.

4. Conclusions

On the basis of our surface morphologies and electrical properties, we presume that the charge carrier

mobility is largely related to the morphology of the organic active layer. We observe that the change trends of the surface morphologies (the average size and the average roughness) of pentacene and RR-P3HT thin films are mutually opposite, as the thickness of the organic layer increases. Further, we demonstrate that the change trends of field-effect mobilities of pentacene and RR-P3HT field-effect transistors are opposite to each other, as the thickness of the organic layer increases within limits.

References

[1] Jaiswal M and Menon R 2006 *Polym. Int.* **55** 1371

[2] Dimitrakopoulos C D and Malenfant P R L 2002 *Adv. Mater.* **14** 99

[3] Sirringhaus H, Tessler N and Friend R H 1998 *Science* **280** 1741

[4] Sirringhaus H, Brown P J, Friend R H, Nielsen M M, Bechgaard K, Langeveld-Voss B M W, Spiering A J H, Janssen R A J, Meijer E W, Herwig P and de Leeuw D M 1999 *Nature* (London) **401** 685

[5] Yuan G C, Xu Z, Zhao S L, Zhang F J, Jiang W W, Song D D, Zhu H N, Li S Y, Huang J Y, Huang H and Xu X R 2008 *Chin. Phys.* B **17** 1887

[6] Kim D H, Park Y D, Jang Y, Yang H, Kim Y H, Han J I, Moon D G, Park S, Chang T, Chang C, Joo M and Ryu C Y 2005 *Adv. Funct. Mater.* **15** 77

[7] Sirringhaus H, Tessler N and Friend R H 1999 *Synth. Met.* **102** 857

[8] Zen A, Plaum J, Hirschmann S, Zhuang W, Jaiser F, Asawapiron U, Rabe J P, Scherf U and Necher D 2004 *Adv. Funct. Mater.* **14** 757

[9] Joshi S, Grigorian S, Pietsch U, Pingel P, Zen A, Neher D and Scherf U 2008 *Macromolecules* **41** 6800

[10] Cho S, Lee K, Yuen J, Wang G, Moses D, Heeger A J, Surin M and Lazzaroni R 2006 *Appl. Phys.* **100** 114503

[11] Kline J R, Mcgehee M D and Toney M F 2006 *Nature* (London) **5** 222

[12] Mcculloch I, Heeney M, Bailey C, Genevicius K, Macdonald I, Shkunov M, Sprarrowe D, Wagnger R, Zhang W, Chabinyc M, Kline R J, Mcgehee M D and Toney M F 2006 *Nature* (London) **5** 328

[13] Yuan G C, Xu Z, Zhao S L, Zhang F J, Huang J Z, Huang J Y, Tian X Y and Xu X R 2008 *Chin. Phys.* B **17** 3822

[14] Kang S J, Noh M, Park D S, Kim H J and Wang C N J 2004 *Appl. Phys.* **95** 2293

[15] Wang G, Hirasa T, Moses D and Heeger A J 2004 *Synth. Met.* **146** 127

[16] Sethuraman K, Ochiai S, Kojima K and Mizutani T 2008 *Appl. Phys. Lett.* **92** 183302

[17] Singh T B and Sariciftci N S 2006 *Annu. Rev. Mater. Res.* **36** 199

[18] Dimitrakopoulos C D and Mascaro D J 2001 *IBM J. Res. & Dev.* **45** 11

[19] Tao C L, Zhang X H, Dong M J, Liu Y Y, Sun Shuo, Ou G P, Zhang F J and Zhang H L 2008 *Chin. Phys.* B **17** 0281